

IM2CAD

Hamid Izadinia
University of Washington

Qi Shan
Zillow Group

Steven M. Seitz
University of Washington



Figure 1: We introduce IM2CAD, a new system that takes a single photograph of a real scene (left), and automatically reconstructs a 3D CAD model (right) that is similar to the real scene.

Abstract

Given a single photo of a room and a large database of furniture CAD models, our goal is to reconstruct a scene that is as similar as possible to the scene depicted in the photograph, and composed of objects drawn from the database. We present a completely automatic system to address this IM2CAD problem that produces high quality results on challenging imagery from real estate web sites. Our approach iteratively optimizes the placement and scale of objects in the room to best match scene renderings to the input photo, used image comparison metrics trained using deep convolutional neural nets. By operating jointly on the full scene at once, we account for inter-object occlusions.

1. Introduction

In his 1963 Ph.D. thesis, Lawrence Roberts [31] demonstrated a system that infers a 3D scene from a single photo (Figure 2). Leveraging a database of known 3D objects, his system analyzed edges in the image to infer the locations and orientations of these objects in the scene. Unlike the vast majority of modern 3D reconstruction techniques, which capture only visible surfaces, Robert’s method was capable of inferring back-facing and occluded surfaces, object segmentations, and recognizes which objects are present.

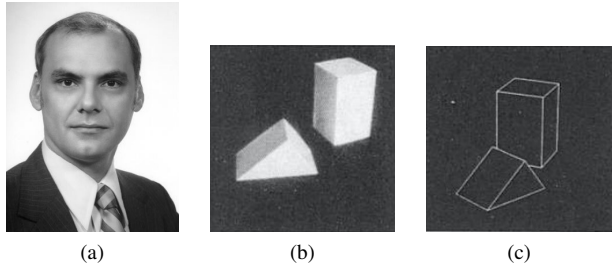


Figure 2: Lawrence Roberts’s (a) 1963 system took an input photo (b) and computed a 3D scene, rendered to a novel viewpoint (c).

While Robert’s method was visionary, more than a half century of subsequent research in computer vision has still not yet led to practical extensions of his approach that work reliably on realistic images and scenes. One major limitation is the need for an accurate, *a priori* 3D model of each object in the scene. While a chair model, e.g., is not hard to come by, obtaining exact 3D models of every chair in the world is not presently feasible. A further challenge is the need to reliably match between features in photographs and CAD models, particularly when the model does not exactly match the object photographed.

We therefore introduce a variant of Robert’s original problem, that we call *IM2CAD*, in which the goal is to re-

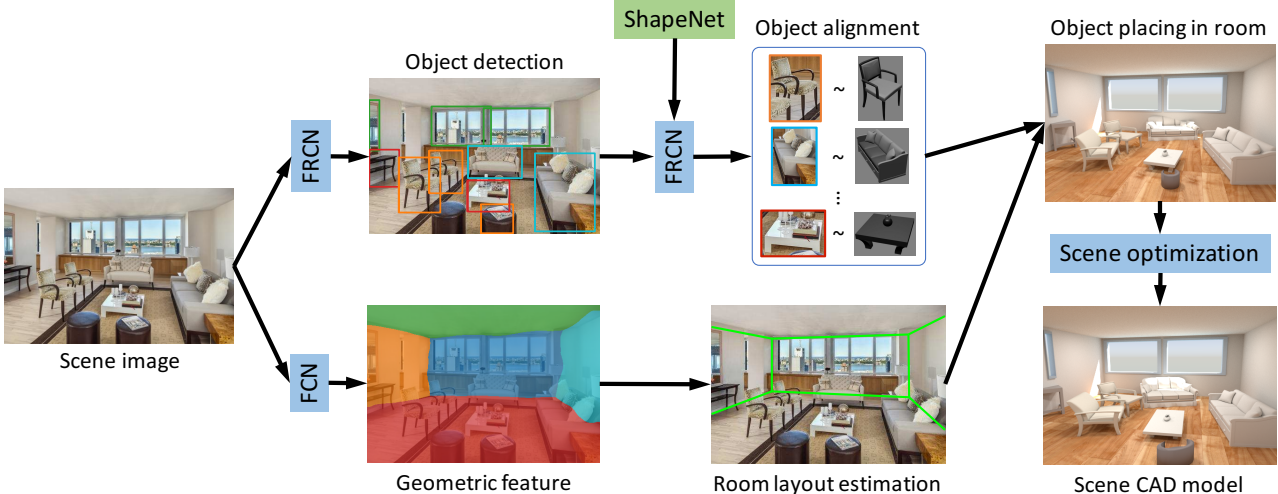


Figure 3: System overview: an input image (left) is processed through a series of steps to produce a Scene CAD model (bottom right).

construct a scene that is **as similar as possible** to the scene depicted in a photograph, where the reconstruction is composed of objects drawn from a database of available 3D object models. For example, the bed in Fig. 1 resembles but does not exactly match the one in the input photograph at left, as we did not have that specific bed in the database. While our results are not perfect, they represent a significant step forward to achieving Robert’s vision on real-world imagery.

Our work builds on a number of recent advances in the computer vision and graphics research community. First, we leverage ShapeNet [5], which contains millions of 3D models of objects, including thousands of different chairs, tables, and other household items. This dataset is a game-changer for 3D scene understanding research, and was key to enabling our work. Second, we use state-of-the-art object recognition algorithms [30] to identify common objects like chairs, tables, windows, etc.; these methods work impressively well in practice. Third, we leverage deep features trained by convolutional neural nets (CNNs) [20] to reliably match between photographs and CAD renderings [3, 19, 33, 17]. Finally, we build on recent research on room reconstruction [14, 21, 25].

Our main contribution is a fully automatic system that produces full-scene CAD models (room + furniture) from a single photo. While many of the technical ingredients of our system draw heavily from prior work (as detailed in the previous paragraph), we also contribute noteworthy technical advances on room modeling and scene optimization. Our room modeling approach produces significant improvement on standard benchmark. And our novel full-scene optimization approach iteratively adjusts the placement and scale of objects to best align rendered photos with input images, operating jointly on the full scene at once, and accounting for inter-object occlusions. Our models include semantics (“ta-

ble”, “chair”), are segmented into objects, and take only a few bytes to represent, encoded as a collection of ShapeNet object IDs and transforms that define position, orientation and scale.

2. Related Work

The last decade has seen renewed interest in single-image 3D modeling, following the work of Hoiem et al., [15] and Saxena et al., [2]. Single-image modeling of indoor scenes has enjoyed significant recent progress, with a series of papers on room-shape estimation (floor, walls, ceiling), e.g., [14, 21, 25] that yield increasingly good results. Our approach for room shape estimation further improves the state of the art.

More recently, researchers have moved beyond walls, and toward approximating furniture in the room using *cuboids* [39, 41, 7, 13, 27]. While the cuboid based approach avoids the need for object databases, the resulting models are primitive and do not accurately depict scene appearance.

Another closely related line of research is 3D object and pose recognition of chairs and other objects [3, 19, 33, 17]. These methods can produce very accurate alignment of a single object to a photograph or depth image. Our work leverages similar 3D object recognition techniques, combined with room shape estimation, to jointly solve for all of the objects in the room in a way that accounts for inter-object occlusions.

Our work also builds upon recent advancements of research on object detection from single images [11, 30].

Producing CAD models of real scenes has applications for VR/AR, games, and education. Its value has been especially well recognized in the real estate industry [10, 8]. Given a set of images, professional 3D artists manually

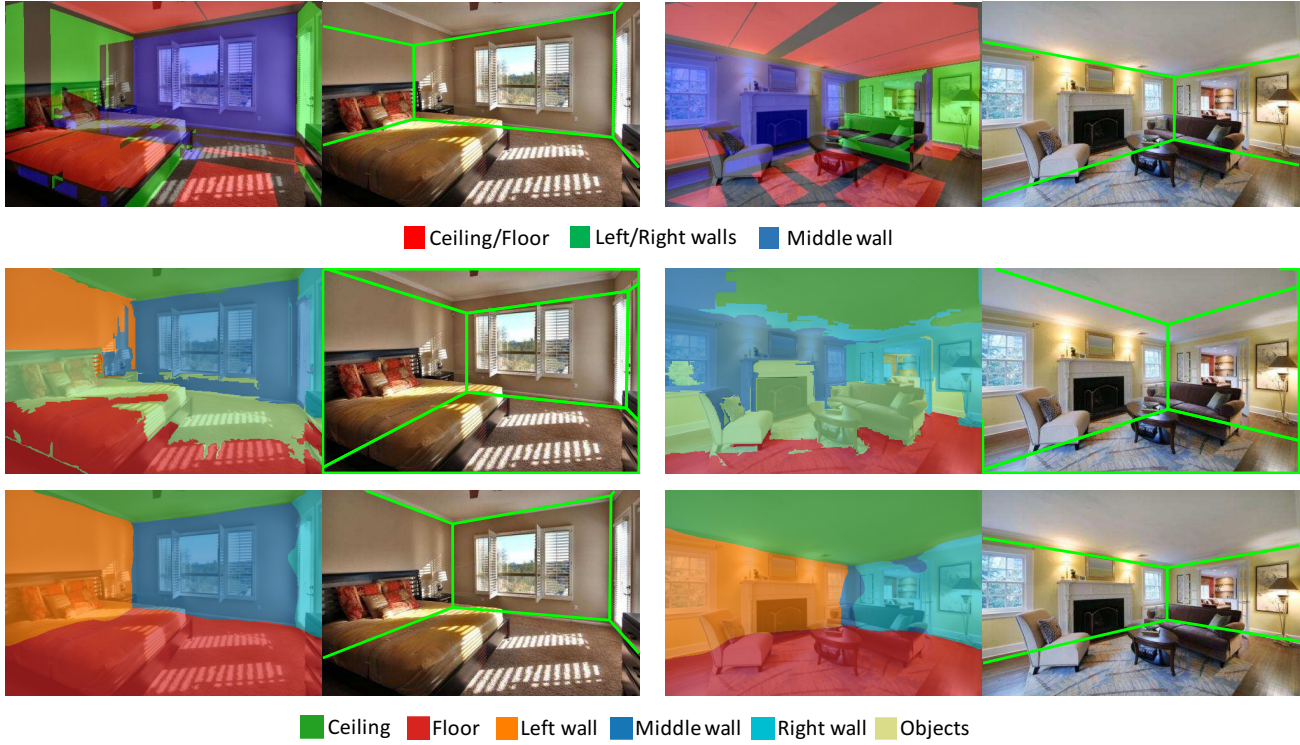


Figure 4: Geometric feature and room layout estimation. Results from (Row1) [21] and (Row2) [14]. Bottom row: our results.

create a 3D CAD model of a property by building out its room layout and placing furniture with roughly approximated scales, locations, and orientations. This process is expensive, time consuming, and difficult to scale. Also, the created CAD models suffer from limited model fidelity as typically they don't reflect the real furniture placement in scenes.

Researchers have explored a variety of techniques to automatically compute CAD scene models using non-photographic means, i.e., using example based approaches [9], utilizing text descriptions [6], and optimizing for furniture arrangements in a given space [40, 26]. These approaches rely on analyzing location and pose correlations between furniture types, based on analyzing databases of scene models. Collecting such data is a challenge, and therefore these approaches can greatly benefit from our solution which generates more comprehensive and plausible indoor models in a fully automatic fashion. Furthermore, our solution is applicable and scalable to industrial applications (e.g., [43]), thanks to the abundance of indoor images available online.

Closest works to ours are [34] and [23] which find the best matching 3D scene model to a given image. But our system is a significant advance in a number of ways. In particular, [34] require a complete scene in the database that matches each image. Hence, their approach can be thought

of as “3D scene retrieval,” whereas we reconstruct each scene from scratch, using a database of furniture (not scene) models. The latter allows for a much broader range of reconstructable scenes and also produces the detailed CAD model of room and furnitures (with their ID in ShapeNet). While [23] do reconstruct the scene by placing individual pieces of furniture, they make a number of limiting assumptions (axis aligned furniture, no walls, easy-to-segment objects), operate on a much smaller database (180 models), and do not demonstrate as broad a range of results (they show less than 10 examples, and mostly furniture with solid color). Both of [34] and [23] use hand-crafted features and [34] specifically learn the weights for each feature dimension via a Support Vector Ranking on images and corresponding 3D scene models, while our proposed method uses CNN feature which is learned end-to-end on just image data. Also, Guo et al. [12] render a synthesized model of the scene using RGBD (depth) images while our method only uses RGB information. The synthesized rooms produced by [12] have low fidelity in terms of object details while we retrieve the detailed ShapeNet CAD model for each object.

Given a single natural image of an indoor scene, our IM2CAD system automatically generates its CAD model by inferring the room geometry, camera parameters, retrieving the CAD model of the scene objects and placing them in the scene with respect to the 3D poses as seen in the in-

put image. We first provide an overview of our approach and motivate the design. Then we will explain the details of each step of our approach.

3. Algorithm

3.1. Overview

Our approach to reconstructing CAD models from an image (see Figure 3) is based on recognizing objects in the scene, inferring room geometry, and optimizing 3D object poses and sizes in the room to best match synthetic renderings to the input photo.

The approach involves several steps, as follows. We first fit room geometry, by classifying pixels as being on walls, floor, or ceiling, and fitting a box shape to the result. In parallel, we detect all of the chairs, tables, sofas, bookshelves, beds, night tables, chest, and windows in the scene using state of the art object detection techniques. Wherever an object, e.g., a bed, is detected with high confidence, we estimate its 3D pose, by comparing its appearance with renderings of hundreds of beds from many different angles, using a deep convolutional distance metric, trained for this purpose. Finally, we optimize for the placement of all objects in the reconstructed room by optimizing the difference between the rendered room and the photograph. Our optimization approach operates on all objects jointly, and thus accounts for inter-object occlusions.

In the remainder of the section, we describe these technical components in detail: room geometry estimation, object detection, object alignment, and scene optimization.

3.2. Room Geometry Estimation

Humans are adept at interpreting the shape of a room (i.e., positions of walls, ceiling, and floor), even in the presence of significant clutter. Computer vision algorithms have also become increasingly good at this task in the last few years by following a paradigm introduced by Hedau et al. [14] and Lee et al. [21] in which a set of room shapes are hypothesized (typically 3D boxes), and evaluated using features in the image.

We improve upon previous approaches to room geometry estimation, by adopting an alternative approach for ranking the room 3D box hypothesis using deep convolutional features. Specifically, we train a network that estimates per-pixel surface labels (ceiling, floor, left, middle, and right walls). These features are analogous to the context geometric feature (“support”, “vertical”, and “sky”) of [16].

Unlike [16] that learns the geometry features from hand-designed low level descriptors (e.g., color, texture, and other perspective cues) over superpixels, our method uses an end-to-end deep Fully Convolutional Network (FCN) [24], using VGG [37] and converting each fully connected layer into a convolutional layer with a kernel covering the en-

Method	Pixel Error(%)
Lee et al. [21]	24.70
Hedau et al. [14]	21.20
Del Pero et al. [27]	16.30
Gupta et al. [13]	16.20
Zhao et al. [42]	14.50
Schwing et al. [35]	13.59
Ramalingam et al. [29]	13.34
Mallya et al. [25]	12.83
Ours	11.13

Table 1: Comparison of room layout pixel misclassification error with best results of different methods on the leading benchmark of [14].

tire input region. Finally, the weights are fine-tuned for the pixel-level labeling task. In this work, we produce the output dense score map of size $41 \times 41 \times 5$ given an input image of 321×321 . We then use upsampling for producing the probability map with the same size of the input image. We trained the FCN network on the annotated indoor scenes in the LSUN dataset [1].

A key advantage of the FCN-based architecture is that it integrates contextual information over the entire image. Whereas most methods use a “distractors” class [14, 25] to remove furniture from consideration, the FCN is able to use furniture as additional context, e.g., using the presence of a bookshelf or bed to infer the likely presence of an adjacent wall. Indeed, Our FCN features (without 3D box estimation) achieve a 12.4% pixel misclassification error compared to 28.9% of [16] on the leading benchmark dataset [14] (see Figure 4).

We note that [25] also use a convolutional network, but rather than classifying surface orientations directly as we do, they estimate informative edges in the scene, and employ a second stage to iteratively re-label room surfaces and rank room box estimates.

When combined with a box-fitting step (we use [21]), we achieve state-of-the-art room estimation results, as shown in Table 1.

3.3. Object Detection

The first step in our furniture modeling pipeline is to detect the presence of objects of interest in the image, and their 2D bounding boxes. While any number of object detectors can be trained, we focused specifically on the following: chair, table, sofa, bookshelf, bed, night table, chest, and window.

Object detection is an area that has seen explosive progress in the last several years, and existing methods work impressively well. In particular, we use the state-of-the-art Faster-RCNN [30] deep network for detection. Faster-RCNN is a unified architecture for both region proposals and object classification with shared convolutional layers.

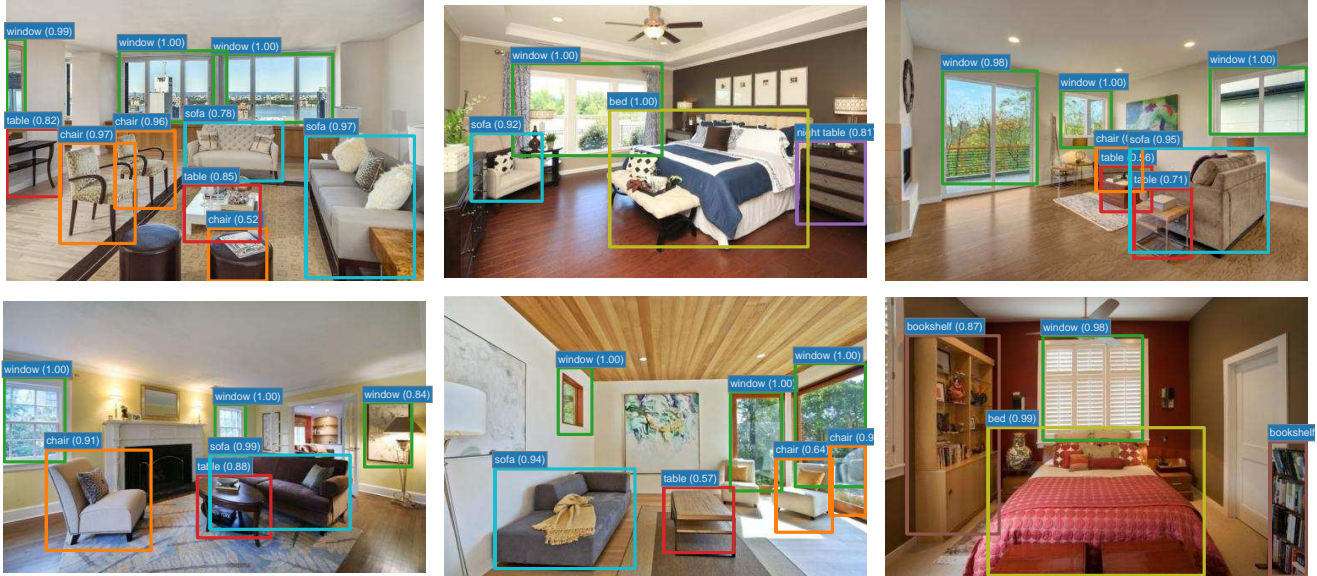


Figure 5: Object detection result on sample images. Each object category is shown with different color. The numbers attached to boxes show the probabilities assigned to each detection.

This network performs two steps to detect objects. First it produces object region proposals, and then it computes the likelihood of each category for the proposed objects using deep convolutional layers. The region proposal layer produces bounding boxes in different scales and aspect ratios. This network is initialized with pre-trained models from large scale object recognition tasks (ILSVRC2012) [18]. The network weights are then fine-tuned for the object proposal and object detection tasks by minimizing an objective function for a multi-task loss on bounding box regression and object misclassification. The trained network is then able to produce bounding boxes with object categories for any image. The network output also includes an object score which shows the probability of that particular object in the bounding box. Greedy non-maximum suppression (NMS) is used to obtain a single peak detection for each object, remove low scoring detections that overlap with higher scoring object bounding boxes.

Our Faster-RCNN implementation uses the VGG16 [37] architecture. We further fine-tune the weights of this network for the object detection task on our eight furniture categories using three publicly available datasets, namely SUN2012 detection dataset [38], ImageNet detection challenge dataset [32], and the window category of Rent3D dataset [22]. We show detection results on a sample of our images in Figure 5.

3.4. CAD Model Alignment

The object detection results from Section 3.3 identify the presence of a “chair” (e.g.,) in a certain region of the image with high probability. Now we wish to determine what *kind* of chair it is, its shape, and approximate 3D pose.

Inspired by [3], we solve this retrieval problem by searching for 3D models that are most similar in appearance to the detected objects in the image. Specifically, we consider all 3D models in the ShapeNet repository [5] associated with our object categories of interest, i.e., chair, table, sofa, bookshelf, bed, night table, chest yielding 9193 models in total. Each 3D model is rendered to 32 quantized viewpoints, consisting of 16 uniformly sampled azimuth angles and two elevation angles (15 and 30 degrees above horizontal).

Robust comparison of photos with CAD models renderings is not straightforward; simple norms like L2 do not work well in practice, due to differences in shape, appearance, shading, and the presence of occluders. We achieve good results, once again, by using convolutional nets; we compute deep features for each of the rendered images and the detected image bounding boxes and use cosine similarity as our distance metric. More specifically, we use the convolution filter response in the ROI-pooling layer of the fine-tuned Faster-RCNN network [30] explained in Section 3.3. A benefit of using the ROI-pooling layer is that the length of its feature vector does not depend on the size and the aspect ratio of the bounding box, thus avoiding the need for non-uniform rescaling (a source of artifacts in general).

Choosing the rendering that best matches each image object detection yields an estimate both for the best-matching CAD model and its approximate 3DOF orientation.

3.5. Object Placement in the Scene

Equipped with a set of CAD models and their approximate orientations, we now wish to place them in the reconstructed room. This placement need not be exact, as we

will further optimize it in a subsequent step, but should be a reasonable initial estimate. To this end, we first estimate the intrinsic camera parameters (K) and camera rotation (R) with respect to the room space using three orthogonal vanishing points [14], and choosing one of the visible room corners as the origin of the world coordinate system. If none of the corners are visible, we choose the origin to be the end point edge boundary of the visible wall intersecting with the floor.

The ShapeNet 3D models are normalized with a bounding box corresponding to a unit cube. Based on the alignment procedure from Section 3.4, we can determine the input photo pixel locations corresponding to each of the eight corners of this cube. We can find the object location and scale in the x and y (parallel to ground plane) directions by intersecting the ground plane with the ray casted from the camera center through the input image pixels corresponding to the bottom four corners of the aligned CAD model cube. To compute the object scale along the z axis, we compute the ratio between the length of the four vertical edges of the projected cube and the length of those edges from the ground plane to the intersection of those lines with the horizontal vanishing line. Note that the height of the vanishing line is equal to the camera height.

We treat windows as a special case, as they are attached to walls instead of the floor. To place windows, we find the intersection of the window bounding box from object detection with each of the walls and assign the window to the wall with which it has the largest overlap. The window’s detected bounding box in the image back-projects to a quadrilateral on the assigned wall. The pose and location of the window is determined by the finding the largest axis-aligned rectangle on the wall plane contained within that quadrilateral.

3.6. Scene Optimization

The placement procedure in Section 3.5 is sensitive to several sources of error including the quantization of object orientations, ground plane misregistration, occlusions, and other factors, which can lead to erroneous estimates of object pose and scale. We therefore propose an optimization in which the configuration of all objects in the scene are jointly aligned. One of the benefits of this procedure is that it properly accounts for inter-object occlusions, and yields much more accurate estimates for object location, scale, and orientation.

After estimating the 3D room geometry and the initial placement of the objects in the scene, we refine our object placements by optimizing the visual similarity of the rendered scene with that of the input image. This optimization is achieved by solving an optimization problem where the variables are the 3D object configurations in the scene and the objective function is the minimization of the cosine dis-

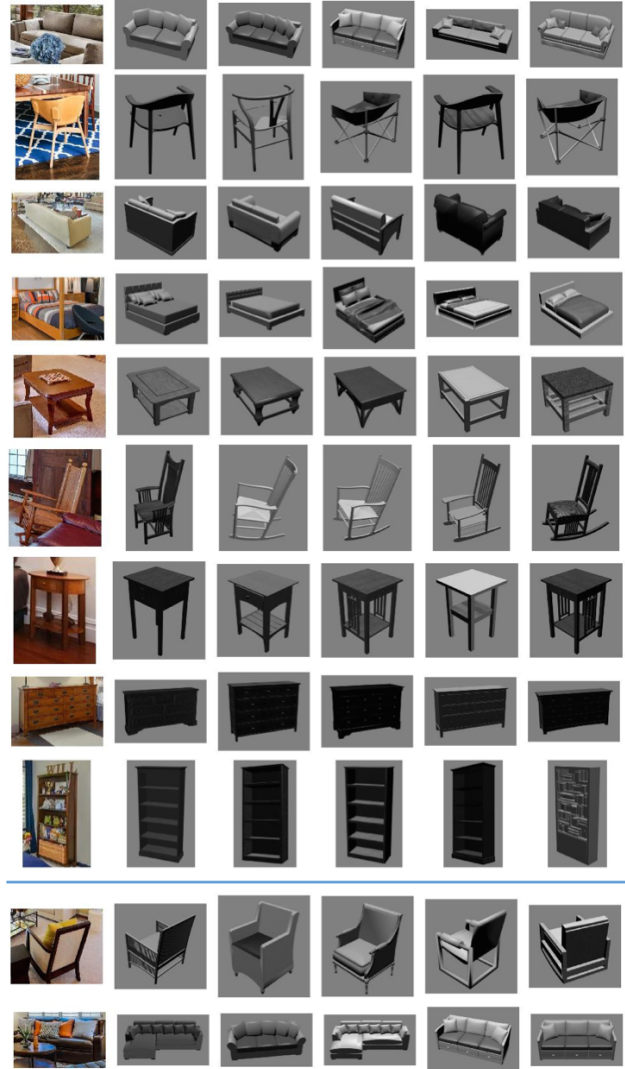


Figure 6: Results of the top five aligned CAD models retrieved for the given object detection bounding box. The retrieved models have similar style and pose with the given object. Last two rows show failure cases: (Row1) visual feature confusion between different poses of the chair, and (Row2) heavy occlusion of sofa by table has made it visually similar to an L-shaped sofa.

tance between the convolutional features obtained from the camera view rendered scene and the input image.

More formally, suppose we detect objects $\{O_1, \dots, O_k\}$ in the scene. The placement of each object O_i is represented by its (x, y, z) location, scale along the x , y and z axis as well as the rotation degree. The variables for all N objects are concatenated into a $7N$ parameter vector. Given a parameter vector, we can generate the rendered image of the scene I^* . The cost function used in our optimization tries to minimize the cosine distance between I^* and the original input image I :



Figure 7: Results of the joint scene optimization step. (Column 1) The initial object placement in the scene. (Columns 2-5) Rendering of the scene in sample iterations during optimization. (Column 5) The last iteration of optimization. (Last column) The objective function error and the optimization convergence. The objective function minimizes dis-similarity between the real and the rendered image. Red dots show the sample iterations that are shown above.

$$\min \Phi(I^*, I) = \frac{1}{|\mathcal{C}|} \sum_{C_i \in \mathcal{C}} 1 - \frac{C_i(I^*) \cdot C_i(I)}{\|C_i(I^*)\| \|C_i(I)\|} \quad (1)$$

We model the feature vector of an image by using the outputs of all convolutional layers¹. In the above equation, \mathcal{C} refers to the set of conv layers in the network and C_i is the feature vector obtained from the i th layer. The total cost function is the average similarity of all layers. The convolutional layers in higher layers of the network provide abstract shape features while the details of the images such as edges and corners appear in the features obtained from the lower layers of the network. The features in higher levels have larger receptive fields, and can therefore cope with larger displacements, and help the optimization to converge in the first iterations when the initial estimates are far off. Similarly, the lower convolutional layers play a greater role in later iterations, to help the objects converge with more precision. In this way, the network provides a natural coarse-to-fine structure to the optimization.

Since our objective function is not differentiable we use COBYLA [28], a derivative free numerical optimization method, deployed in a Python optimization package. We found this procedure to work very well in practice. Figure 7 shows the convergence of the method for example scenes.

4. Coloring CAD models

We use the median color of each object in the input image for scene optimization (Section 3.6) and visualization. The process is as follows. First, we project the best aligned CAD model of an object onto its bounding box in the image. Now the goal is to find a median color from these pixels inside the projected mask, and use that as the object color. As true median is undefined for multi-dimensional data, in this case three dimensions (RGB), we compute an approximated

¹We used conv1-1, conv1-2, conv2-1, conv2-2, conv3-1, conv3-2, conv3-3, conv4-1, conv4-2, conv4-3, conv5-1, conv5-2 and conv5-3 layers in the VGG network

geometric median. To be more specific, we find the median value of each color channel separately, and take the closest color which appears within the mask. We also compute the median color for each wall of the room using a similar approach. We compute the mask of each wall through the room geometry, and exclude the bounding boxes from detected objects. In our experiments, this approach works well for scene optimization and creates visually pleasant renderings without falling into the uncanny valley [36] (see results in Figures 9 and 10).

5. Results

We evaluated the proposed IM2CAD system with 100 real world indoor images collected from “Zillow Digs” [43]. These images are living room and bedroom shots as our training object category consists of chair, table, sofa, bookshelf, bed, night table, chest, and window, typical bedroom and living room furnitures. We cover a variety of room styles from traditional, contemporary, to modern. We find “Zillow Digs” a good source of evaluating our system as its images present furniture arrangement, complexity, and cluttering in real world scenes.

Our IM2CAD approach consistently produces reasonable results on most of the test images. Figures 9 and 10 are representative of the top 30% of our results, where most of the furniture is detected, represented using well-matched CAD models, and properly posed. Typical failure results are shown in Figure 8. Our failures are rarely catastrophic, and generally fall into the category of some furniture items being omitted or misplaced.

Object pose estimation can sometimes get stuck in local optimal. Notice that the foreground chair in Figure 8(a) is in an incorrect pose while the chair legs are aligned almost perfect to the image. Please also notice that in Figure 6, the last two rows demonstrate the cases where the visual similarity fails to retrieve appropriate CAD models. Heavily occluded objects impose additional challenges. Notice the missing chair and coffee table in Figure 8(a) and (b). If the



Figure 8: Failure cases: inaccurate chair pose (a); mis-detection of a chair (a) and table (b); non-cubic room shape (c).

room shape is not a perfect cubical (Figure 8(c)), our room layout estimation fits the best cube to the room and failed to recover the true room shape. The windows can be confused with paintings as they have very similar visual features (see Figures 9 and 10). Both windows and paintings typically appear as glassy and shiny rectangular shapes on a wall.

In our experiments, we use the Caffe [18] framework to implement and train our deep networks. The object detection and geometric feature extraction are processed on a Titan X GPU, while the room layout sampling and object pose estimation are computed over on CPU. For a typical input image of size 500×300 , the computational time is approximately: 0.15 seconds on object detection, 0.3 seconds on geometric feature extraction, 8 seconds on room layout sampling and ranking, and 10 seconds on object placement. Our scene optimization is an iterative process where each iteration takes about 1 second. We set the maximum number of iterations to be 250. Therefore, the overall CAD model creation process finishes within 5 minutes.

To produce final room renderings with global illumination, we use Blender Cycle Render Engine [4], with fixed lighting consisting of distant sunlight from the top right point and five area lights on the ceiling. The final rendering process takes about 15 minutes with global illumination.

6. Conclusion

This paper presents a fully automatic system that reconstructs a 3D CAD model of an indoor scene from a single photograph, by utilizing a large database of 3D furniture models. It estimates room geometry, detects, and aligns objects in the image with highly accurate 3D poses. We present innovative approaches on room modeling and scene optimization, which are keys to the success of our system. We evaluate on a wide range of real world living room and bedroom photographs with a variety of home styles. The results demonstrate the effectiveness of our approach, particularly in creating 3D CAD models that faithfully resemble the real scenes. With the abundance of indoor photographs available online, our system is ready to produce an extremely large database of indoor scene models.

Our system does have notable limitations, and inspires a number of areas for future work. We assume the room geometry in the image can be modeled with part of a cube. Understandably, heavily occluded objects impose challenges. Working with complicated room geometry is an

area of future improvement. We assume objects are always on the ground plane (e.g., chairs and beds) or attached to walls (windows), posing a lamp on a table would require extension of our work. Incorporating more object types will benefit our system to create more faithful scene models. Currently, the object category does not cover rooms like kitchens and bathrooms. It would be interesting to extend the framework to more room types, if quite challenging.

References

- [1] Lsun room layout estimation dataset. <http://lsun.cs.princeton.edu/>, 2015. 4
- [2] A. Y. N. Ashutosh Saxena, Sung H. Chung. Learning depth from single monocular images. In *NIPS*, 2005. 2
- [3] M. Aubry, D. Maturana, A. Efros, B. Russell, and J. Sivic. Seeing 3D chairs: exemplar part-based 2D-3D alignment using a large dataset of cad models. In *CVPR*, 2014. 2, 5
- [4] Blender. Blender cycles render engine. <https://www.blender.org/manual/en/render/cycles/index.html>. 8
- [5] A. X. Chang, T. Funkhouser, L. Guibas, P. Hanrahan, Q. Huang, Z. Li, S. Savarese, M. Savva, S. Song, H. Su, J. Xiao, L. Yi, and F. Yu. ShapeNet: An Information-Rich 3D Model Repository. Technical Report arXiv:1512.03012 [cs.GR], 2015. 2, 5
- [6] A. X. Chang, M. Savva, and C. D. Manning. Learning spatial knowledge for text to 3d scene generation. In *EMNLP*, 2014. 3
- [7] W. Choi, Y.-W. Chao, C. Pantofaru, and S. Savarese. Indoor scene understanding with geometric and semantic contexts. *IJCV*, 2015. 2
- [8] DIAKRIT. DIAKRIT International. <http://www.diakrit.com/>. 2
- [9] M. Fisher, D. Ritchie, M. Savva, T. Funkhouser, and P. Hanrahan. Example-based synthesis of 3d object arrangements. *TOG*, 31(6):135, 2012. 3
- [10] Floored. Floored. <http://www.floored.com/>. 2
- [11] R. Girshick, J. Donahue, T. Darrell, and J. Malik. Rich feature hierarchies for accurate object detection and semantic segmentation. In *CVPR*, 2014. 2

[12] R. Guo, C. Zou, and D. Hoiem. Predicting complete 3d models of indoor scenes. *arXiv preprint arXiv:1504.02437*, 2015. 3

[13] A. Gupta, M. Hebert, T. Kanade, and D. M. Blei. Estimating spatial layout of rooms using volumetric reasoning about objects and surfaces. In *NIPS*, 2010. 2, 4

[14] V. Hedau, D. Hoiem, and D. Forsyth. Recovering the spatial layout of cluttered rooms. In *ICCV*, 2009. 2, 3, 4, 6

[15] D. Hoiem, A. A. Efros, and M. Hebert. Automatic photo pop-up. In *SIGGRAPH*, 2005. 2

[16] D. Hoiem, A. A. Efros, and M. Hebert. Recovering surface layout from an image. *IJCV*, 2007. 4

[17] Q. Huang, H. Wang, and V. Koltun. Single-view reconstruction via joint analysis of image and shape collections. In *SIGGRAPH*, 2015. 2

[18] Y. Jia, E. Shelhamer, J. Donahue, S. Karayev, J. Long, R. Girshick, S. Guadarrama, and T. Darrell. Caffe: Convolutional architecture for fast feature embedding. In *Proceedings of the ACM International Conference on Multimedia*, 2014. 5, 8

[19] N. Kholgade, T. Simon, A. Efros, and Y. Sheikh. 3D object manipulation in a single photograph using stock 3d models. In *SIGGRAPH*, 2014. 2

[20] A. Krizhevsky, I. Sutskever, and G. E. Hinton. Imagenet classification with deep convolutional neural networks. In *NIPS*. 2012. 2

[21] D. C. Lee, M. Hebert, and T. Kanade. Geometric reasoning for single image structure recovery. In *CVPR*, 2009. 2, 3, 4

[22] C. Liu, A. G. Schwing, K. Kundu, R. Urtasun, and S. Fidler. Rent3d: Floor-plan priors for monocular layout estimation. In *CVPR*, 2015. 5

[23] Z. Liu, Y. Zhang, W. Wu, K. Liu, and Z. Sun. Model-driven indoor scenes modeling from a single image. In *Proceedings of the 41st Graphics Interface Conference*, 2015. 3

[24] J. Long, E. Shelhamer, and T. Darrell. Fully convolutional networks for semantic segmentation. In *CVPR*, 2015. 4

[25] A. Mallya and S. Lazebnik. Learning informative edge maps for indoor scene layout prediction. In *ICCV*, 2015. 2, 4

[26] P. Merrell, E. Schkufza, Z. Li, M. Agrawala, and V. Koltun. Interactive furniture layout using interior design guidelines. In *SIGGRAPH*, 2011. 3

[27] L. D. Pero, J. Bowdish, D. Fried, B. Kermgard, E. Hartley, and K. Barnard. Bayesian geometric modeling of indoor scenes. In *CVPR*, 2012. 2, 4

[28] M. J. Powell. A direct search optimization method that models the objective and constraint functions by linear interpolation. In *Advances in optimization and numerical analysis*. 1994. 7

[29] S. Ramalingam, J. Pillai, A. Jain, and Y. Taguchi. Manhattan junction catalogue for spatial reasoning of indoor scenes. In *CVPR*, 2013. 4

[30] S. Ren, K. He, R. Girshick, and J. Sun. Faster r-cnn: Towards real-time object detection with region proposal networks. In *NIPS*, 2015. 2, 4, 5

[31] L. G. Roberts. *Machine perception of three-dimensional soups*. PhD thesis, Massachusetts Institute of Technology, 1963. 1

[32] O. Russakovsky, J. Deng, H. Su, J. Krause, S. Satheesh, S. Ma, Z. Huang, A. Karpathy, A. Khosla, M. Bernstein, A. C. Berg, and L. Fei-Fei. ImageNet Large Scale Visual Recognition Challenge. *IJCV*, 2015. 5

[33] R. Salas-Moreno, R. Newcombe, H. Strasdat, P. Kelly, and A. Davison. Slam++: Simultaneous localisation and mapping at the level of objects. In *CVPR*, 2013. 2

[34] S. Satkin, M. Rashid, J. Lin, and M. Hebert. 3dnn: 3d nearest neighbor. *IJCV*, 2015. 3

[35] A. G. Schwing and R. Urtasun. Efficient exact inference for 3d indoor scene understanding. In *ECCV*, 2012. 4

[36] J. Seyama and R. S. Nagayama. The uncanny valley: Effect of realism on the impression of artificial human faces. *Presence*, 16(4):337–351, 2007. 7

[37] K. Simonyan and A. Zisserman. Very deep convolutional networks for large-scale image recognition. *arXiv preprint arXiv:1409.1556*, 2014. 4, 5

[38] J. Xiao, J. Hays, K. A. Ehinger, A. Oliva, and A. Torralba. Sun database: Large-scale scene recognition from abbey to zoo. In *CVPR*, 2010. 5

[39] J. Xiao, B. Russell, and A. Torralba. Localizing 3D cuboids in single-view images. In *NIPS*, 2012. 2

[40] L.-F. Yu, S.-K. Yeung, C.-K. Tang, D. Terzopoulos, T. F. Chan, and S. J. Osher. Make it home: automatic optimization of furniture arrangement. In *SIGGRAPH*, 2011. 3

[41] Y. Zhang, S. Song, P. Tan, and J. Xiao. PanoContext: A whole-room 3d context model for panoramic scene understanding. In *ECCV*, 2014. 2

[42] Y. Zhao and S.-C. Zhu. Scene parsing by integrating function, geometry and appearance models. In *CVPR*, 2013. 4

[43] Zillow. Zillow Digs. <http://www.zillow.com/digs/>. 3, 7



Figure 9: The reconstruction results. In each example the left image is the real input image and the right image is the rendered 3D CAD model produced by IM2CAD.



Figure 10: The reconstruction results. In each example the left image is the real input image and the right image is the rendered 3D CAD model produced by IM2CAD (Continue).